



# Deglaciation records of $^{17}\text{O}$ -excess in East Antarctica: reliable reconstruction of oceanic normalized relative humidity from coastal sites

R. Winkler<sup>1</sup>, A. Landais<sup>1</sup>, H. Sodemann<sup>2</sup>, L. Dümbgen<sup>3</sup>, F. Prié<sup>1</sup>, V. Masson-Delmotte<sup>1</sup>, B. Stenni<sup>4</sup>, and J. Jouzel<sup>1</sup>

<sup>1</sup>Laboratoire des Sciences du Climat et de l'Environnement (LSCE/IPSL/CEA/CNRS/UVSQ), UMR8212, Orme des Merisiers, 91191 Gif-sur-Yvette, France

<sup>2</sup>Institute for Atmospheric and Climate Science, Swiss Federal Institute of Technology Zürich, Universitätsstrasse 16, 8092 Zürich, Switzerland

<sup>3</sup>Department of Mathematics and Statistics, Institute of Mathematical Statistics and Actuarial Science, University of Bern, Alpeneggstrasse 22, 3012 Bern, Switzerland

<sup>4</sup>Department of Geosciences, University of Trieste, Via E. Weiss 4, 34127 Trieste, Italy

Correspondence to: R. Winkler (renato.winkler@lsce.ipsl.fr)

Received: 20 May 2011 – Published in Clim. Past Discuss.: 10 June 2011

Revised: 10 November 2011 – Accepted: 16 November 2011 – Published: 3 January 2012

**Abstract.** We measured  $\delta^{17}\text{O}$  and  $\delta^{18}\text{O}$  in two Antarctic ice cores at EPICA Dome C (EDC) and TALDICE (TD), respectively, and computed  $^{17}\text{O}$ -excess with respect to VSMOW. The comparison of our  $^{17}\text{O}$ -excess data with the previous record obtained at Vostok (Landais et al., 2008a) revealed differences up to 35 ppm in  $^{17}\text{O}$ -excess mean level and evolution for the three sites. Our data show that the large increase depicted at Vostok (20 ppm) during the last deglaciation is a regional and not a general pattern in the temporal distribution of  $^{17}\text{O}$ -excess in East Antarctica. The EDC data display an increase of 12 ppm, whereas the TD data show no significant variation from the Last Glacial Maximum (LGM) to the Early Holocene (EH). A Lagrangian moisture source diagnostic revealed very different source regions for Vostok and EDC compared to TD. These findings combined with the results of a sensitivity analysis, using a Rayleigh-type isotopic model, suggest that normalized relative humidity ( $\text{RH}_n$ ) at the oceanic source region (OSR) is a determining factor for the spatial differences of  $^{17}\text{O}$ -excess in East Antarctica. However,  $^{17}\text{O}$ -excess in remote sites of continental Antarctica (e.g. Vostok) may be highly sensitive to local effects. Hence, we consider  $^{17}\text{O}$ -excess in coastal East Antarctic ice cores (TD) to be more reliable as a proxy for  $\text{RH}_n$  at the OSR.

## 1 Stable water isotopes in the hydrological cycle

The stable isotopes  $^2\text{H}/\text{H}$  and  $^{18}\text{O}/^{16}\text{O}$  ratios of water molecules in ice cores have been used for several decades as proxies for past temperature over the polar regions and have permitted the reconstruction of past climate changes over the last 800 ka (ka = thousand years before present) in Antarctica (Jouzel et al., 2007). Their link with temperature results from isotopic fractionation of water at each phase transition in the water cycle and especially along the water mass trajectory from the region of evaporation to the final polar precipitation site. The combination of  $\delta^2\text{H}$  and  $\delta^{18}\text{O}$  leads to the second order parameter  $d$ -excess =  $\delta^2\text{H} - 8 \delta^{18}\text{O}$  (Dansgaard, 1964). It has been shown that  $d$ -excess in ice/snow from polar regions is mainly a function of temperature at the oceanic moisture source region (OSR) (Ciais and Jouzel, 1994; Petit et al., 1991), but it also depends on normalized relative humidity ( $\text{RH}_n$ ) at the OSR (Jouzel et al., 1982), the surface ocean isotopic composition, wind speed and finally the temperature at the precipitation site (e.g. Stenni et al., 2001 and 2010; Vimeux et al., 2002). The dependence of  $d$ -excess on these different parameters is variable from one site to another (Masson-Delmotte et al., 2008; Vimeux et al., 1999), and it is thus difficult to infer quantitative information on climatic conditions at the evaporative regions from  $d$ -excess alone.

Angert et al. (2004) suggested that another second order parameter provided by the combination of  $\delta^{17}\text{O}$  and  $\delta^{18}\text{O}$  in  $^{17}\text{O}$ -excess =  $\ln(\delta^{17}\text{O} + 1) - 0.528\ln(\delta^{18}\text{O} + 1)$  of ice cores would provide additional information on humidity conditions of the OSR. The expected signal from  $^{17}\text{O}$ -excess is very small, of the order of 10–40 ppm, and thus difficult to measure accurately. Note that in previous studies, the unit permeg instead of ppm was used, but here we use ppm to be consistent with the SI system (Coplen, 2011). Progress in analytical devices have allowed Barkan and Luz (2005) to measure  $\delta^{17}\text{O}$  and  $\delta^{18}\text{O}$  with a sufficiently high precision to calculate  $^{17}\text{O}$ -excess of water samples. Their laboratory study also showed that  $^{17}\text{O}$ -excess should not depend on OSR temperature. Extending the theoretical approach developed by Craig and Gordon (1965) and Merlivat and Jouzel (1979) to link  $d$ -excess and conditions prevailing at the OSR, one can derive that  $^{17}\text{O}$ -excess and  $\text{RH}_n$  of the OSR are linearly related with decreasing  $^{17}\text{O}$ -excess for increasing  $\text{RH}_n$ . This expected negative correlation has recently been monitored in situ (surface water vapour) over the Southern Ocean by Uemura et al. (2010).

Landais et al. (2008a) identified an increase of  $^{17}\text{O}$ -excess from 20 to 40 ppm between the Last Glacial Maximum (LGM, 21 ka) and Early Holocene (EH, 8 ka) in the Vostok ice core in East Antarctica. They attributed this 20 ppm increase to a decrease in  $\text{RH}_n$  of 20 % over the Vostok OSR. However, a 20 % decrease in  $\text{RH}_n$  over the ocean (from LGM to EH) appears large and is not supported by atmospheric general circulation models (GCM), which simulate unchanged ocean surface  $\text{RH}_n$  over glacial/interglacial periods (Risi et al., 2010).

The work of Landais et al. (2008a) raised the question if the deglacial increase at Vostok in  $^{17}\text{O}$ -excess is a local signal or if it is a more regional pattern that could be observed at other sites in Antarctica. Here, we address this question by analysing the temporal variations of  $^{17}\text{O}$ -excess over the last deglaciation (21 to 9 ka) at two other sites in East Antarctica with very different climatic conditions: EPICA Dome C (EDC) and Talos Dome (TD).

The ice cores of EDC and TD provide both continuous and high quality information about the past climate. EDC (75°06' S, 123° E) is characterised by continental climatic conditions (present-day annual mean temperature:  $-54.5^\circ\text{C}$ ) and a very low accumulation rate of about  $25\text{ kg m}^{-2}\text{ a}^{-1}$ . The geographical location and the climatic conditions at the drilling site of EDC are comparable to those at Vostok (78° 27' S, 106° 50' E), although Vostok is slightly colder and drier with a temperature of  $-55.3^\circ\text{C}$  and an accumulation rate of about  $21.5\text{ kg m}^{-2}\text{ a}^{-1}$  (Masson-Delmotte et al., 2011). TD (72° 49' S, 159° 11' E) is situated in the coastal area of East Antarctica and is marked by higher temperature ( $-40.1^\circ\text{C}$ ) and much higher accumulation rate of  $80\text{ kg m}^{-2}\text{ a}^{-1}$  (Stenni et al., 2011).

In this article, we first give a short summary of the definitions used for the triple isotopic composition of oxygen in

water as well as an overview of the different fractionation effects in the hydrological cycle. Then, we present the  $^{17}\text{O}$ -excess profiles obtained on the EDC and TD ice cores. A statistical analysis is performed to test the significance of glacial/interglacial shifts (Appendix A). To help with the interpretation of the different water isotopic profiles, we use the classical simple isotopic model adapted to the description of water isotopes in Antarctica (Mixed Cloud Isotopic Model, hereafter MCIM – Ciais and Jouzel, 1994). We perform sensitivity studies with various configurations of the supersaturation parameter of the MCIM to discuss the different influences on  $^{17}\text{O}$ -excess on coastal and continental East Antarctic ice cores over the last deglaciation.

## 2 Fractionation processes in the triple isotopic composition of oxygen in meteoric water

### 2.1 Equilibrium fractionation

During each phase-change in the water cycle, fractionation of stable water isotopes occurs. Two different kinds of fractionation are distinguished. The first one is called equilibrium fractionation: for water molecules containing heavy oxygen or hydrogen isotopes, the water vapour pressure is lower than for the abundant (light) water molecules. For this reason, water molecules which contain  $^{17}\text{O}$ ,  $^{18}\text{O}$  or deuterium stay preferably in the condensed phase compared to the lightest  $\text{H}_2^{16}\text{O}$  molecules. To quantify isotopic fractionation, the equilibrium fractionation factor  $\alpha_{\text{eq}}$  has been introduced.  $\alpha_{\text{eq}}$  varies with temperature and was theoretically determined for the different water isotopes by Van Hook (1968). In addition,  $\alpha_{\text{eq}}$  for  $\frac{\text{H}_2^{18}\text{O}}{\text{H}_2^{16}\text{O}}$  for liquid-vapour ( $^{18}\alpha_{\text{eq-liqu-vap}}$ ) was measured by Majoube (1971a) for temperatures between 0 and  $100^\circ\text{C}$ . The equilibrium fractionation coefficient for solid-vapor ( $^{18}\alpha_{\text{eq-sol-vap}}$ ) was also determined experimentally for temperatures between 0 to  $-33.4^\circ\text{C}$  (Majoube, 1971b). The equilibrium fractionation factor associated with  $\frac{\text{H}^2\text{H}^{16}\text{O}}{\text{H}_2^{16}\text{O}}$  was measured by Merlivat and Nief (1967) for the temperature range of 0 to  $-40^\circ\text{C}$  for ice-vapour and of 0 to  $-15^\circ\text{C}$  for liquid-vapour. The equilibrium fractionation factor ( $^{17}\alpha_{\text{eq-liqu-vap}}$ ) associated with  $\frac{\text{H}_2^{17}\text{O}}{\text{H}_2^{16}\text{O}}$  was measured by Barkan and Luz (2005) for liquid-vapour over the temperature range of 11.4 to  $41.5^\circ\text{C}$ . For negative temperature, we rely on theoretical calculations performed by Van Hook (1968) of the ratio between  $\ln(^{17}\alpha_{\text{eq-vap-sol}})/\ln(^{18}\alpha_{\text{eq-vap-sol}})$ ; he obtained values of 0.529 to 0.5285 for temperatures between 0 and  $-40^\circ\text{C}$ . Recent measurements of water vapour and precipitation in Greenland (Landais et al., 2011) provide confidence in the application of these fractionation factors for polar regions.

## 2.2 Kinetic fractionation

The second kind of fractionation is due to the different molecular diffusivities and is called kinetic fractionation (Mook, 1994). The fractionation factor for kinetic fractionation  $\alpha_{\text{kin}}$  is a function of molecular diffusivity  $D$  of the considered isotopes. The ratios  $^{18}\text{D}/^{16}\text{D}$  and  $^2\text{HD}/^{16}\text{D}$  (where  $^{18}\text{D}$  and  $^2\text{HD}$  refer to the diffusion constants of the heavy water isotope  $\text{H}_2^{18}\text{O}$  and  $^2\text{HH}^{16}\text{O}$  in the gaseous phase, respectively) were measured by Merlivat (1978) and Cappa et al. (2003), who obtained significantly different results. Barkan and Luz (2007) and Luz et al. (2009) confirmed the results of Merlivat (1978) and performed the first experimental measurements of the relative diffusivity of  $\text{H}_2^{17}\text{O}$  vs.  $\text{H}_2^{16}\text{O}$  in air.

## 2.3 Definition of $^{17}\text{O}$ -excess

For a triple isotopic system, the relationship between the isotopic ratios  $^{17}\text{R}$  and  $^{18}\text{R}$  (\*R =  $\frac{*}{16}\text{O}$ , \* referring to  $^{17}\text{O}$  or  $^{18}\text{O}$ , respectively) is governed by a power law (Eq. 1) (Mook and Grotes, 1973; Craig, 1957):

$$\frac{^{17}\text{R}_s}{^{17}\text{R}_r} = \left( \frac{^{18}\text{R}_s}{^{18}\text{R}_r} \right)^\lambda \quad (1)$$

where the subscripts s and r refer, respectively, to the sample and reference. Starting from Eq. (1), Miller (2002) introduced a logarithmic definition for the  $^{17}\text{O}$ -anomaly, denoted as  $\Delta^{17}\text{O}$ :

$$\ln(\Delta^{17}\text{O} + 1) = \ln(\delta^{17}\text{O} + 1) - \lambda \ln(\delta^{18}\text{O} + 1). \quad (2)$$

The advantage of this logarithmic notation is that fractionation lines are straight lines in a  $\ln(\delta^{17}\text{O} + 1)$  vs.  $\ln(\delta^{18}\text{O} + 1)$  plot, while they are curved in a  $\delta^{17}\text{O}$  vs.  $\delta^{18}\text{O}$  plot (Luz and Barkan, 2004). Moreover, although the absolute value of the  $^{17}\text{O}$ -anomaly, using the above definition, depends on the isotopic composition of the reference material, the slope  $\lambda$  of the fractionation line in a  $\ln(\delta^{17}\text{O} + 1)$  vs.  $\ln(\delta^{18}\text{O} + 1)$  plot does not.

Meijer and Li (1998) analysed the triple isotopic composition of many different natural waters and determined the exponent  $\lambda$  of Eq. (1). They found a value of  $0.5281 \pm 0.0015$ . This number seems to be valid for all meteoric waters (Meijer and Li, 1998) and therefore  $^{17}\text{O}$ -excess was defined by Barkan and Luz (2007) as:

$$^{17}\text{O-excess} = \ln(\delta^{17}\text{O} + 1) - 0.528 \ln(\delta^{18}\text{O} + 1). \quad (3)$$

The number of 0.528 in Eq. (3) is called the slope of the global meteoric waterline for the system of  $\ln(\delta^{17}\text{O} + 1)$  vs.  $\ln(\delta^{18}\text{O} + 1)$ . An analogy can be drawn with the  $\delta^2\text{H}$  vs.  $\delta^{18}\text{O}$  system where the slope of the global meteoric waterline is 8:  $\delta^2\text{H} = 8\delta^{18}\text{O} + 10\text{‰}$  (Craig, 1961) – and leads to  $d$ -excess definition ( $d$ -excess =  $\delta^2\text{H} - 8\delta^{18}\text{O}$ ) (Dansgaard, 1964).

## 2.4 Evaporation

During the process of evaporation over the ocean, equilibrium and kinetic fractionation contribute simultaneously to the lower value of  $\delta^{17}\text{O}$  and  $\delta^{18}\text{O}$  of the water vapour with respect to  $\delta^{17}\text{O}$  and  $\delta^{18}\text{O}$  of the ocean. The ratio between the fractionation factors differs for equilibrium fractionation ( $\ln^{17}\alpha_{\text{eq}}/\ln^{18}\alpha_{\text{eq}} = 0.529$ ) and for kinetic fractionation ( $\ln \frac{^{17}\text{D}}{^{16}\text{D}}/\ln \frac{^{18}\text{D}}{^{16}\text{D}} = 0.518$ ). Relatively stronger kinetic fractionation leads to an increase of  $^{17}\text{O}$ -excess in the water vapour. The relative contribution of kinetic fractionation to the total fractionation process at evaporation is negatively correlated to  $\text{RH}_n$  at the site of evaporation. As a consequence, variations of  $^{17}\text{O}$ -excess in the evaporate over the OSR are directly related to changes in  $\text{RH}_n$  at the ocean surface with:

$$^{17}\text{O-excess} = -\ln(^{18}\alpha_{\text{eq}}^{0.529} \ ^{18}\alpha_{\text{diff}}^{0.518} (1 - \text{RH}_n) + \text{RH}_n) + 0.528 \ln(^{18}\alpha_{\text{eq}} \ ^{18}\alpha_{\text{diff}} (1 - \text{RH}_n) + \text{RH}_n) \quad (4)$$

where the exponent-coefficients of 0.518 and 0.529, are respectively based on the experiments of Barkan and Luz (2005, 2007).  $^{18}\alpha_{\text{diff}} = \left(\frac{^{18}\text{D}}{^{16}\text{D}}\right)^n$ , where the exponent  $n$  varies between 0 (turbulent wind regime) to 1 (laminar wind regime) (Mook, 1994; Merlivat and Jouzel, 1979).  $^{18}\alpha_{\text{diff}}$  was determined in wind tunnel experiments by Merlivat and Jouzel (1979) ( $^{18}\alpha_{\text{diff}} = 1.006$ ) and inferred by Uemura et al. (2010) from isotopic measurements in water vapour above the surface of the Southern Ocean ( $^{18}\alpha_{\text{diff}} = 1.008$ ).  $\text{RH}_n$  is the relative humidity normalized at the ocean surface temperature (e.g. Gat and Mook, 1994). Note that a similar influence of  $\text{RH}_n$  at evaporation on  $d$ -excess of the evaporate is predicted because of the strong differences between  $(^2\text{H}\alpha_{\text{eq}} - 1)/(^{18}\alpha_{\text{eq}} - 1) (\approx 8)$  and  $(\frac{^{16}\text{D}}{^2\text{HD}} - 1)/(\frac{^{16}\text{D}}{^{18}\text{D}} - 1) (\approx 0.88)$  when taking the Merlivat (1978) diffusion coefficients.

## 3 Method

### 3.1 Experimental method

In order to measure both  $\delta^{17}\text{O}$  and  $\delta^{18}\text{O}$  in ice core samples from EDC and TD, we used the water fluorination technique as introduced by Barkan and Luz (2005). 2  $\mu\text{l}$  of water are injected, under a continuous helium flux ( $20 \text{ ml min}^{-1}$ ), into a heated ( $370^\circ\text{C}$ ) nickel-tube, which is filled with  $\text{CoF}_3$  where the water-molecule is split into  $\text{O}_2$  and hydrofluoric acid (HF). HF is trapped with liquid nitrogen at the exit of the nickel tube. The gaseous  $\text{O}_2$  is then trapped in a stainless steel manifold which is immersed in a liquid helium tank. After 40 min the manifold is connected to a Dual Inlet Mass-spectrometer (ThermoFisher Delta V) where  $\delta^{17}\text{O}$  and  $\delta^{18}\text{O}$  are measured at the same time. Each IRMS measurement contains two runs. During each run, the ratio between the sample and the working standard ( $\text{O}_2$ -gas) is

determined 16 times. We also measure daily our laboratory water-standard, which is calibrated against VSMOW, using the same fluorination- and IRMS-methods. The analytical uncertainty associated with each sample (3 to 4 replica) correspond to the pooled standard deviation

$$\sigma_p = \sqrt{\frac{\sum_{i=1}^k (n_i - 1) s_i^2}{\sum_{i=1}^k (n_i - 1)}} \quad (5)$$

where  $n_i$  is the number of replicas of the  $i$ -th sample (3 to 4),  $s_i$  is the standard deviation of the  $i$ -th sample and  $k$  is the total number of samples. The pooled standard deviation is 6.4 ppm for the 58 EDC data-points and 6.2 ppm for the 44 TD data-points.

Since measurements of  $^{17}\text{O}$ -excess are of magnitude ppm, small peculiarities of the water fluorination technique or the IRMS may result in significant inter laboratory offsets. We thus compared 5 working standards spanning the entire range of our measurements between our laboratory (LSCE) and the Institute of Earth Sciences in Jerusalem (IES). The largest difference in  $^{17}\text{O}$ -excess between the two laboratories was observed for the two extreme standards VSMOW ( $\delta^{18}\text{O} = 0\text{‰}$ ) and Dome F ( $\delta^{18}\text{O} = -58.2\text{‰}$ ). We observed increasing differences (max. 22 permeg) between the two laboratories for decreasing  $\delta^{18}\text{O}$ . By definition, VSMOW has a  $^{17}\text{O}$ -excess of 0 ppm. The Dome F internal standard, which is made of surface snow from the site of Dome Fuji in Antarctica (made by Osamu Abe), was measured with  $^{17}\text{O}$ -excess = 1 ppm at the IES (Luz and Barkan, 2009) and with a  $^{17}\text{O}$ -excess of 23 ppm at LSCE (during the course of our measurements). Since the fractionation coefficients associated with  $\delta^{17}\text{O}$  were measured at the IES, we decided to correct our  $^{17}\text{O}$ -excess measurements performed at LSCE with respect to the results obtained at the IES using the inter calibration of our working standards. We shifted our  $^{17}\text{O}$ -excess results by 22 permeg for the EDC data and by 15 permeg for the TD data.

In order to ensure the reliability of the applied correction, we remeasured a selection of samples of the of the previously at IES analysed Vostok record. Figure 1 shows this comparison between measurements (12 samples) performed by Landais et al. (2008a) at IES and the same samples remeasured at LSCE. Most (10 out of 12 samples) measurements are consistent within the analytical uncertainty of  $\pm 6$  ppm. Evaporation during storage (samples at IES were not stored at  $-20$ , but at  $0^\circ\text{C}$ ) is likely the explanation for the two outliers. Although we compared only a small number of samples, we still depicted an increasing  $^{17}\text{O}$ -excess trend during the last deglaciation, which corresponds well to the trend observed by Landais et al. (2008a). Therefore, we feel confident to reliably compare our  $^{17}\text{O}$ -excess records obtained at LSCE with the previous ones published in Landais et al. (2008a). The details of inter calibration of working standards between

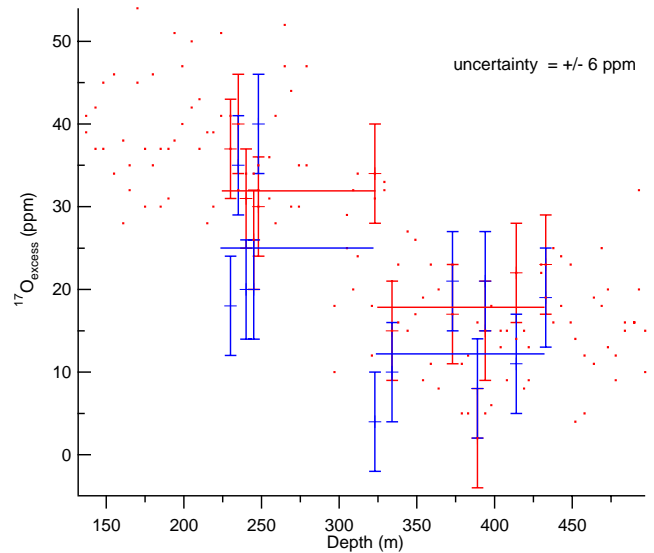


**Fig. 1.** Comparison of  $^{17}\text{O}$ -excess measurements conducted at the Institute of Earth Science (IES) in Jerusalem and LSCE. We measured at LSCE (blue)  $^{17}\text{O}$ -excess of 12 samples of the Vostok ice-core, previously measured by Landais et al. (2008a) at IES (red). Apart from two data points, the replica conducted at LSCE match (within the uncertainty of  $\pm 6$  ppm) the previously obtained data. The blue lines represent the mean levels of the replica for EH (5 samples) and LGM (7 samples), respectively. The red lines are the corresponding mean values previously obtained at the IES. At LSCE, we measured a glacial/interglacial shift of 12 ppm, which corresponds very well to the increase (14 ppm for this data-subset) depicted by Landais et al. (2008a).

different laboratories will be discussed in a technical paper, which is in preparation.

### 3.2 Mixed Cloud Isotopic Model (MCIM)

In order to compare the different mean levels and evolution of  $^{17}\text{O}$ -excess (and  $d$ -excess) in continental (Vostok, EDC) and coastal (TD) Antarctic regions, we performed several sensitivity experiments with the mixed cloud isotopic model (MCIM) (Ciais and Jouzel, 1994). Among other models (Kavanaugh and Cuffey, 2003; Johnsen et al., 1989; Noone, 2008), we chose this model because up to now, it is one of the most efficient in simulating the evolution of  $\delta^{18}\text{O}$ ,  $d$ -excess and  $^{17}\text{O}$ -excess in remote Antarctica. It has been widely used to interpret  $d$ -excess and  $\delta^{18}\text{O}$  variations in ice cores (Stenni et al., 2010; Masson-Delmotte et al., 2004; Vimeux et al., 2001; Stenni et al., 2001). This model has been extended to include fractionation factors  $^{17}\alpha$  for  $\text{H}_2^{17}\text{O}$  and was used by Landais et al. (2008a) to interpret the variations of  $^{17}\text{O}$ -excess over the last deglaciation on the Vostok ice core as a change of  $\text{RH}_n$  at the OSR.

The MCIM is based on a Rayleigh distillation (Merlivat and Jouzel, 1979; Jouzel and Merlivat, 1984). It describes the

isotopic composition of the condensed phase (liquid water or ice) and the water vapour at each step between the OSR and the precipitation site on the ice sheet. To determine the isotopic composition of the first water vapour over the ocean surface, the assumption that all the evaporated water will return to the ocean as rain (“closure assumption”) is made. This assumption is true in nature, but only globally. Locally, one can not assume that all evaporated water will return to the same ocean basin (e.g. Delmotte et al., 2000; Jouzel and Koster, 1996). However, a more sophisticated model study (Risi et al., 2010) using a single column model in the evaporative regions, instead of the closure assumption, showed that the dependency of  $^{17}\text{O}$ -excess in polar ice on  $\text{RH}_n$  remains the same as with the MCIM and does not challenge the interpretation of the  $^{17}\text{O}$ -excess variations in the Vostok ice core proposed by Landais et al. (2008a).

During the formation of liquid, only equilibrium fractionation occurs. Depending on temperature, the MCIM allows in the zone of “mixed cloud” the coexistence of liquid droplets and ice crystals. In this zone, the Bergeron-Findeisen process associated with kinetic fractionation effects is taken into account (Ciais and Jouzel, 1994). The formation of snow crystals is a non-equilibrium process and the fractionation factor is a function of  $\alpha_{\text{eq}}$  and  $\alpha_{\text{kin}}$ :

$$\alpha = \alpha_{\text{eq}}\alpha_{\text{kin}} \quad (6)$$

The relative proportion of kinetic fractionation is governed by the supersaturation function in the cloud, which is (Jouzel and Merlivat, 1984):

$$\alpha_{\text{kin}} = \frac{S}{1 + \alpha_{\text{eq}}\left(\frac{D}{*D}\right)(S-1)} \quad (7)$$

$D$  and  $*D$  correspond to the diffusion constants for the light and the heavy isotopes, respectively. As in previous studies (Landais et al., 2008a; Petit et al., 1991; Jouzel and Merlivat, 1984), we described  $S$  as a linear function of temperature:  $S = p + qT_c$ , where  $T_c$  is the temperature in the cloud in  $^{\circ}\text{C}$  for every time step of the distillation process.  $p$  and  $q$  are tunable parameters (see Sect. 4.3).

### 3.3 Forcing and tuning of the MCIM

The model is prescribed by initial parameters such as the temperature ( $T_{\text{source}}$ ),  $\text{RH}_n$ , wind speed and pressure of the source region as well as the isotopic composition of the ocean and the condensation temperature ( $T_c$ , assumed to be linearly related to the surface temperature, Ekaykin and Lipenkov, 2009) and pressure at the precipitation site. There are several tuning parameters (Ciais and Jouzel, 1994) such as the dependence of supersaturation on temperature ( $S = p + qT_c$ ), the fraction of condensate remaining in the cloud, the temperature range where liquid and solid water can coexist, a coefficient ( $\gamma$ ) that determines the proportion of the re-evaporation of liquid phase, and the parameter that controls at what temperature the first ice forms. For the tuning of the model, we

used the same method as in previous studies with  $\delta^{17}\text{O}$ ,  $\delta^{18}\text{O}$  and  $\delta^2\text{H}$  (Landais et al., 2008a, Masson-Delmotte et al., 2005; Vimeux et al., 1999, 2001; Stenni et al., 2001; Stenni et al., 2003; Stenni et al., 2010). We adjusted the tuning parameters to obtain the best simulations of the  $^{17}\text{O}$ -excess and  $d$ -excess evolution with  $\delta^{18}\text{O}$  over an Antarctic transect (Terra Nova Bay – Dome C; Landais et al., 2008a). The second constraint for our tuning was to reproduce the  $\delta^{18}\text{O}$ ,  $d$ -excess and  $^{17}\text{O}$ -excess values of the EH for the 3 sites on which we concentrate here. For this, we performed  $\delta^{18}\text{O}$ ,  $d$ -excess and  $^{17}\text{O}$ -excess simulations for each of the sites (Vostok, EDC and TD) taking into account their different OSR with different  $\text{RH}_n$  and temperature. This second constraint was not used in previous studies because they concentrated only on one site. Such tuning with one single supersaturation function for all the different sites is a compromise to best fit most of the data and we are aware that this leads to model-data mismatches in some areas (e.g. TD). In a second step, we also performed sensitivity studies using different supersaturation functions  $S$  and increased reevaporation of the liquid phase ( $\gamma$ ) in the cloud (Fig. 3a and b and Table 1).

### 3.4 Lagrangian moisture source diagnostics

The moisture sources for precipitation at the drilling sites Vostok, EDC and TD have been determined from the Lagrangian moisture source diagnostic of Sodemann et al. (2008) using data from a 5.5-yr Lagrangian simulation with 1.4 million particles filling a global domain and covering the period October 1999 to April 2005 (Stohl and Sodemann, 2009). The simulation was conducted with the Lagrangian particle dispersion model FLEXPART (Stohl et al., 2005), which has the advantage over conventional trajectory calculations that turbulent air parcel motions are represented by parametrisations. Evaporation into and precipitation from tracked air parcels have been identified along their trajectories from changes in specific humidity within and above the boundary layer, and have been made quantitative by weighting according to the evaporation-precipitation sequence as described in Sodemann et al. (2008). Here, moisture sources for the Vostok, EDC and TD ice core sites are based on particles precipitating within a 200 km radius around each site. Since Central Antarctica is one of Earth’s most arid regions, all specific humidity changes in the vicinity of each site larger than  $0.02 \text{ g kg}^{-1}$  within 6 h have been assumed to be due to precipitation. The threshold to identify moisture uptakes is the same as in Stohl and Sodemann (2009), with  $0.1 \text{ g kg}^{-1}$  within 6 h. Due to the sparsity of observational data and the very dry conditions, the moisture diagnostic is at its limits of applicability here, in particular for SH winter conditions and for individual ice core sites. Seasonal averaging over the period of the simulation, however, results in a sufficiently robust simulation result to assume that the identified moisture source patterns are meaningful. Note that clear sky precipitation (diamond dust), a special feature of high

**Table 1.** Output of the MCIM model, using the tuning that best fits the  $^{17}\text{O}$ -excess and  $d$ -excess data ( $d$ ), obtained on the transect from Terra Nova Bay to EDC (Landais et al., 2008a) and the isotopic values of EH at Vostok, EDC and TD.  $S = 1 - 0.0033 T_c$  (figures in brackets show an example of an alternative tuning with  $S = 1 - 0.004 T_c$ ) corresponds to the supersaturation function. OSRs were determined using the results of the back trajectory study (Appendix B, Sodemann et al., 2008 and Sodemann and Stohl, 2009). The model input  $T_{\text{source}}$  and  $\text{RH}_n$  for the three different sites were obtained by the use of NCEP-map <http://www.esrl.noaa.gov/>. The analytical uncertainty for the  $\delta^{18}\text{O}$  measurements is 0.05 ‰ and 0.7 ‰ for  $d$ -excess (EPICA Members, 2004; Stenni et al., 2010, 2001 and Vimeux et al., 1999). The uncertainty for the  $^{17}\text{O}$ -excess measurements is 6.4 ppm for EDC and 6.2 ppm for TD, respectively.

	Model						Measurements		
	$T_{\text{site}}$ (°C)	$T_{\text{source}}$ (°C)	$\text{RH}_n$	$\delta^{18}\text{O}$ (‰)	$^{17}\text{O}$ -ex (ppm)	$d$ (‰)	$\delta^{18}\text{O}$ (‰)	$^{17}\text{O}$ -ex (ppm)	$d$ (‰)
Vostok	-55.3	17	0.8	-53 (-51)	50 (37)	15 (11)	-56	40	15
Dome C	-54.5	17	0.8	-51 (-50)	50 (38)	13 (10)	-50.7	23	9.3
Talos Dome	-40.1	15	0.9	-38(-37.5)	38 (35)	-3 (-2)	-36.6	2.6	2.6

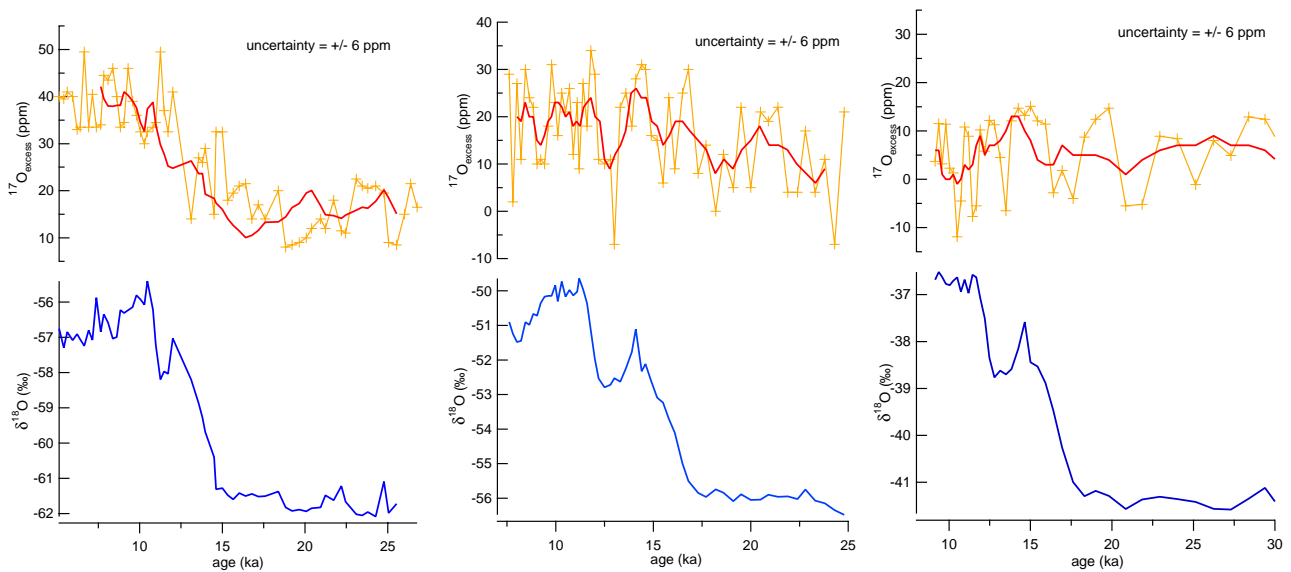


**Fig. 2.** Upper panel: record of  $^{17}\text{O}$ -excess during the last deglaciation for the ice core sites of Vostok (a) from Landais et al. (2008a), EDC (b) and TD (c). The thick red lines represent a 5 point moving average. The temporal resolution of the data corresponds to about 2 data points per 1000 yr. Lower panel (blue): Here we present  $\delta^{18}\text{O}$  values which were measured earlier by equilibration method; the Vostok data are from Vimeux et al. (1999), while the EDC data were published by EPICA-Members (2004) and more recently the TD data by Stenni et al. (2010). Our  $\delta^{18}\text{O}$  measurements done by the fluorination method are not presented here, but are in agreement within  $\pm 0.5$  ‰ with previous measurements (most of the difference is explained by a storage effect).

latitude precipitation that may be a seasonally relevant contributor to accumulation at Vostok and EDC, is not taken into account in the underlying model simulations. Appendix B discusses the results of the moisture source diagnostic in detail.

## 4 Results

### 4.1 Temporal distribution of $^{17}\text{O}$ -excess at Vostok, EPICA Dome C (EDC) and Talos Dome (TD)

Figure 2a to c displays the records of  $^{17}\text{O}$ -excess and  $\delta^{18}\text{O}$  during the last deglaciation from Vostok, EDC and TD ice cores ( $\delta^{18}\text{O}$ -references: Vimeux et al., 1999; EPICA-Members, 2004; and Stenni et al., 2001; Stenni et al., 2003). The  $^{17}\text{O}$ -excess data from Vostok were obtained at IES and published in Landais et al. (2008a). The  $^{17}\text{O}$ -excess records

from EDC and TD were obtained at LSCE. The thick lines represent a 5 point moving average. During the period from LGM to EH,  $^{17}\text{O}$ -excess increases by about 20 ppm for the Vostok site. Our  $^{17}\text{O}$ -excess results of EDC show an increase of 12 ppm. For TD we do not evidence any clear trend over the last deglaciation and  $^{17}\text{O}$ -excess stays around a mean level of 5 ppm for the whole period.

## 4.2 Statistical analysis

At first sight, it is not evident to draw robust conclusions on the temporal evolution of  $^{17}\text{O}$ -excess at EDC and TD, since the scattering of the data is quite large. We performed a statistical analysis of our data in order to check if the mean  $^{17}\text{O}$ -excess levels for LGM and EH significantly differ. For simplicity, we mention in this section only the conclusions of this analysis. The detailed description being given in the Appendix A.

First, we compared the  $^{17}\text{O}$ -excess mean values of LGM and EH for the sites of EDC and TD. Significance was tested by computing the two-sample confidence bounds, which yielded a higher  $^{17}\text{O}$ -excess mean level for EH compared to LGM for the site of EDC, but not for TD. Since this test contains only a limited number of data points (which correspond to the period of LGM and EH, respectively), it does not provide a tool to reproduce the trend of  $^{17}\text{O}$ -excess during the complete period. So, in a second step we performed a regression analysis which includes all data points of the considered records at EDC and TD (58 data points for EDC and 44 for TD). Several fit functions with different degrees of freedom were tested (F-tests) and the most robust one was obtained when using a linear function. The result of the linear fit for the EDC-data was an increase of 12 ppm during the period from LGM to EH. In contrast, no significant temporal gradient of  $^{17}\text{O}$ -excess was obtained for TD (Fig. A1a and b in Appendix A).

## 4.3 Results and limits of the MCIM

Table 1 displays the results of MCIM simulation for the three sites of our studies after adjustment of the tuning parameters to best fit the  $\delta^{18}\text{O}$ ,  $^{17}\text{O}$ -excess and  $d$ -excess on the transect Terra Nova Bay – Dome C and the mean isotopic values of EH at Vostok, EDC and TD.

We can make the following statements:

1. The  $\delta^{18}\text{O}$  data are well reproduced by the MCIM for EDC and TD. The difference between data and modelled  $\delta^{18}\text{O}$  for Vostok is higher (3 ‰) than the differences at EDC and TD, respectively.
2. The modelled  $d$ -excess corresponds rather well to the data and the relative variation for the sites of Vostok and EDC. However,  $d$ -excess is 5.6 ‰ too low for TD.
3. The MCIM reproduces well the  $^{17}\text{O}$ -excess level at Vostok as well as the relative variation between EDC and

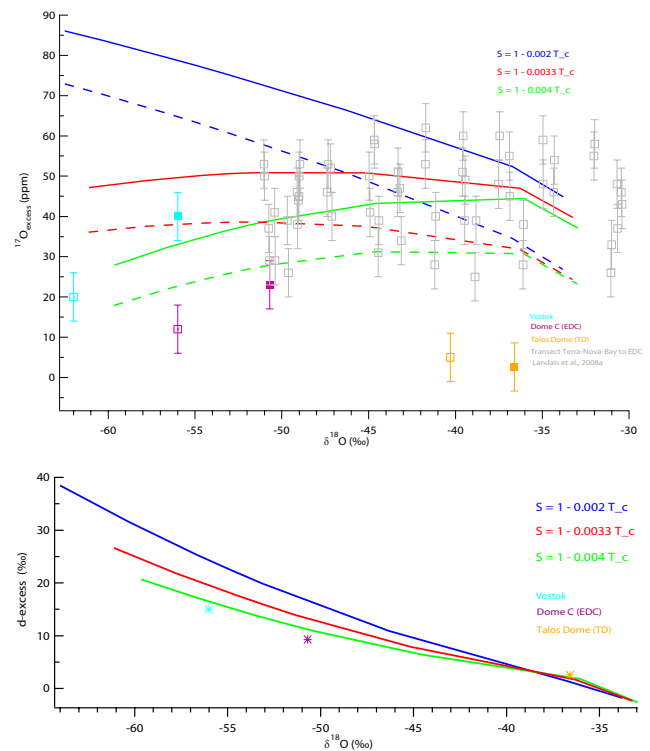


**Fig. 3.** Dependency of  $^{17}\text{O}$ -excess (a), upper panel on supersaturation  $S$  as a function of  $\delta^{18}\text{O}$  (with fixed climatic parameters,  $\text{RH}_n$ ,  $T_{\text{source}}$  and  $T_{\text{site}}$ ). The different coloured lines represent different  $S$ . The dashed lines represent  $S$ , but with 10 times more re-evaporation (gamma) of the liquid phase in the cloud. The filled symbols are the EH values and the empty ones are the LGM values of  $^{17}\text{O}$ -excess (analytical uncertainty =  $\pm 6$  ppm). The light grey dots are the data of the transect study from Terra Nova Bay to EDC (Landais et al., 2008a). (b) (lower panel): dependency of  $d$ -excess on  $S$  as a function of  $\delta^{18}\text{O}$  (with fixed climatic parameters,  $\text{RH}_n$ ,  $T_{\text{source}}$  and  $T_{\text{site}}$ ). The coloured lines represent different  $S$ . Data points (star-symbols) for EH stem from (EPICA Members, 2004; Stenni et al., 2010, 2004, 2001; Vimeux et al., 1999)

TD. The modelled  $^{17}\text{O}$ -excess is 20 to 30 ppm too high for EDC and TD, compared to the data.

4. Modification of the supersaturation function  $S$  (e.g.  $S = 1 - 0.004 T_c$ ) can improve the agreement between, e.g. modelled and measured  $d$ -excess (EDC and TD), and can also lead to a better fit to  $^{17}\text{O}$ -excess data for Vostok and EDC (Table 1). However, such a tuning would produce almost the same  $^{17}\text{O}$ -excess (35 to 38 ppm) for all three sites, which is not consistent with the evidenced relative variation between the different sites. Furthermore, only the tuning with  $S = 1 - 0.0033 T_c$  is compatible with the stable  $^{17}\text{O}$ -excess on the Antarctic transect (Fig. 3a).

It is not surprising to obtain such a discrepancy between some observations and the MCIM outputs. Indeed, the

MCIM (Ciais and Jouzel, 1994) has first been dedicated to interpret water isotopic profiles at Vostok, and previous studies (Masson-Delmotte et al., 2008, Vimeux et al., 2001) always used different tunings for different sites. We thus expect that the MCIM, with one single tuning configuration, cannot capture the different patterns of isotopic distillation all over Antarctica. Yet our goal was not to reproduce very precisely the absolute values of the data, but to better understand the influence of the climatic parameters ( $\text{RH}_n$ ,  $T_{\text{site}}$  and  $T_{\text{source}}$ ) on  $d$ -excess and  $^{17}\text{O}$ -excess to interpret their changes over the deglaciation. Therefore, we chose one single supersaturation function in order to disentangle the influence of the climatic parameters ( $\text{RH}_n$ ,  $T_{\text{site}}$  and  $T_{\text{source}}$ ) on the modelled  $^{17}\text{O}$ -excess from the influence of  $S$ . In a second step, we varied different tuning parameters (Fig. 3a and b) in order to investigate quantitatively the change of sensitivity of the isotopic ratios to the climatic parameters. We give some examples of these sensitivity studies below:

1. We performed dozens of sensitivity studies varying the following tuning parameters: fraction of condensate remaining in the cloud, the temperature range where liquid and solid water can coexist, and the parameter which controls at what temperature the first ice forms. We found that they do not change the sensitivity of  $d$ -excess and  $^{17}\text{O}$ -excess to the climatic parameters ( $\text{RH}_n$ ,  $T_{\text{site}}$  and  $T_{\text{source}}$ ) significantly. Note also that wind speed has no significant impact on our findings.
2. We increased the proportion of re-evaporation ( $\gamma$ ) of the liquid phase in the cloud by a factor of 10. The dashed lines in Fig. 3a show that this test decreases the level of  $^{17}\text{O}$ -excess by 10 to 18 ppm, which brings in better agreement the data and model output. In tandem, it leads to an increase of the sensitivity of  $^{17}\text{O}$ -excess to  $T_{\text{source}}$  and  $\text{RH}_n$  by almost 100 % and 20 %, respectively, but no change in the sensitivity of  $^{17}\text{O}$ -excess to local climatic conditions ( $T_{\text{site}}$ ). In contrast, the same change of the re-evaporation scheme of the low latitudes does not influence the sensitivity of  $d$ -excess (which is strongly affected by  $T_{\text{site}}$ ) to source climatic parameters  $T_{\text{source}}$  and  $\text{RH}_n$ . This test is not necessarily realistic, but it shows that  $^{17}\text{O}$ -excess of ice is recording climate changes in the low latitudes more directly than  $d$ -excess.
3. We found that the sensitivity of  $^{17}\text{O}$ -excess and  $d$ -excess to  $T_{\text{site}}$  depends almost entirely on the tuning of the supersaturation function  $S$ , which we adjusted as for the transect study (Terra Nova Bay – EDC):  $S = 1 - 0.0033 T_c$ . Figure 3a shows that the tuning of supersaturation with temperature ( $\delta^{18}\text{O}$ ) is more important for the remote sites of Vostok and EDC ( $\delta^{18}\text{O}$  between  $-50$  to  $-62$ ‰), where supersaturation is expected to be higher. At Vostok and EDC,  $^{17}\text{O}$ -excess glacial/interglacial shift can be as different as  $-9$  ppm

( $S = 1 - 0.004 T_c$ ) to  $+6$  ppm ( $S = 1 - 0.002 T_c$ ), hence 15 ppm difference. In contrast, for TD, the shift varies from  $-0.5$  ppm to  $+6$  ppm, which is not more than our analytical uncertainty. The above sensitivity of  $^{17}\text{O}$ -excess to supersaturation tuning highlights the importance of mapping  $^{17}\text{O}$ -excess spatial variations for different periods (LGM, EH, ...) to help constrain isotopic fractionation during snow formation.

We carried out no studies concerning the sensitivity of the  $d$ -excess and  $^{17}\text{O}$ -excess to the fractionation factors  $^{17}\alpha$ ,  $^{18}\alpha$  and  $^{2}\text{H}\alpha$ . If we would have used the ratio of the diffusion constants (see Sect. 2.2) obtained by Cappa et al. (2003) instead of Merlivat (1978), it would mainly affect the sensitivity of  $d$ -excess to climatic conditions. Below we summarize the output of our sensitivity studies in a linear equation, which represents the span of the sensitivities of each climatic parameter. Only the supersaturation has been strongly tuned, as described above.

$$\begin{aligned} \Delta^{17}\text{O} - \text{excess} &= -(86 \text{ to } 110)\Delta\text{RH}_n \\ &- (-0.2 \text{ to } 0.5)\Delta T_{\text{site}} + (0.34 \text{ to } 0.61)\Delta T_{\text{source}} \\ \Delta d - \text{excess} &= -(4.5 \text{ to } 9.5)\Delta\text{RH}_n \\ &- (1.29 \text{ to } 2.04)\Delta T_{\text{site}} + (1.31 \text{ to } 1.5)\Delta T_{\text{source}} \\ &- 3\Delta\delta^{18}\text{O}_{\text{ocean}} \end{aligned} \quad (8)$$

The dependency of  $\Delta d$ -excess on the isotopic composition of the ocean ( $\delta^{18}\text{O}_{\text{ocean}}$ ) has been obtained as depicted in Jouzel et al. (2003). This coefficient depends only on the isotopic composition ( $\delta^{18}\text{O}$  and  $\delta^2\text{H}$ ) of the polar site of interest. Its absolute value increases with decreasing  $\delta^2\text{H}$  or  $\delta^{18}\text{O}$ .  $\Delta\delta^{18}\text{O}_{\text{ocean}}$  does not change  $^{17}\text{O}$ -excess due to its logarithmic definition (Landais et al., 2009).

The coefficients obtained in Eq. (8) are rather close to what was obtained previously by Landais et al. (2009) or Risi et al. (2010) for the Vostok site.  $^{17}\text{O}$ -excess mainly depends on OSR  $\text{RH}_n$ ; the relatively high sensitivity of  $^{17}\text{O}$ -excess to  $T_{\text{source}}$  is only obtained in an unrealistic case of very high re-evaporation of the liquid phase in the cloud. The modelled variations of  $d$ -excess with climatic conditions at the source are also comparable with the previous studies of Vimeux et al. (2001) and Stenni et al. (2001). However, as already discussed in Landais et al. (2009) and Risi et al. (2010), the sensitivity of  $d$ -excess with  $T_{\text{site}}$  increases especially on the central Antarctic sites, because of the tuning of the supersaturation imposed by the stability of  $^{17}\text{O}$ -excess on the Antarctic transect.

## 5 Discussion

1. From the comparison of the three Antarctic profiles, we conclude that the Antarctic  $^{17}\text{O}$ -excess evolution over the deglaciation displays strong regional differences. In

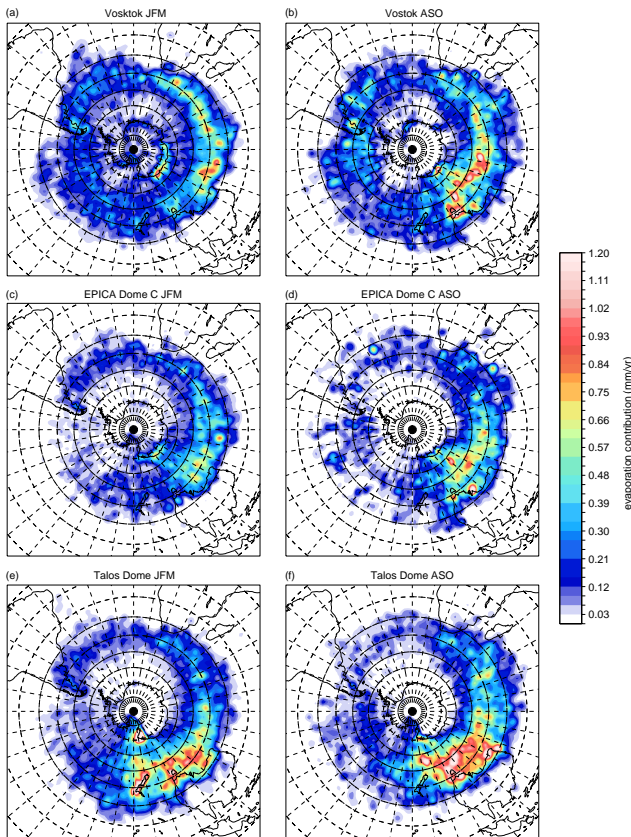


**Fig. 4.** Seasonal mean moisture sources for the ice core drilling sites Vostok during (a) January-February-March (JFM) and (b) August-September-October (ASO). (c) EPICA Dome C during JFM and (d) ASO, (e) Talos Dome during JFM and (f) ASO. Shading shows the contribution of surface evaporation to precipitation in the target area in units of  $\text{mm yr}^{-1}$ .

particular, the strong increase at Vostok is not observed with the same magnitude at the site of EDC and no shift is detected at the more coastal site of TD. The first conclusion from this study is that the  $^{17}\text{O}$ -excess signal recorded at Vostok (Landais et al., 2008a) is a signal with regional peculiarities that cannot be generalized to all Antarctica.

- From the three sites presented here, we note a clear modern spatial gradient of the  $^{17}\text{O}$ -excess mean level at EH from the more coastal site (TD, 2.6 ppm) to the most remote one (Vostok, 40 ppm), EDC being associated with an intermediate  $^{17}\text{O}$ -excess level (23 ppm). This evolution from the coast to the East Antarctic plateau is different from the  $^{17}\text{O}$ -excess evolution measured over a transect on the same region of Antarctica (Landais et al., 2008a), which does not exhibit any clear trend from the coast to central East Antarctica.

- We propose an explanation for the unequal mean levels of  $^{17}\text{O}$ -excess at EH and for the different trends over the deglaciation for the 3 sites based on the MCIM detailed above. From the MCIM outputs (Eqs. 8), we can exclude unequal  $T_{\text{source}}$  as an explanation for different  $^{17}\text{O}$ -excess mean levels and trends. In contrast, source  $\text{RH}_n$  can have a strong influence.

The large difference in  $^{17}\text{O}$ -excess (up to 35 ppm) between the continental sites of Vostok and EDC compared to the coastal one at TD can partly be explained by site specific OSRs with different  $\text{RH}_n$  for the two regions (Vostok- and EDC- $\text{RH}_n = 80\%$ , TD- $\text{RH}_n = 90\%$ ), as indicated by the findings of the back trajectory model (Fig. 4 and Appendix B). The difference of 17 ppm between  $^{17}\text{O}$ -excess mean levels at Vostok and EDC is more compelling. The sparsity of precipitation events makes it difficult to distinguish (using the back trajectory model) the moisture origin of Vostok from the one of EDC. Still, we propose that higher  $d$ -excess and  $^{17}\text{O}$ -excess at Vostok may be due to different OSRs and moisture trajectories. Indeed, the Lagrangian moisture source diagnostics revealed stronger influences of the Pacific and Atlantic sectors for Vostok, compared to EDC, where moisture is mainly coming from the western Indian Ocean sector (Fig. 4; Appendix B; Sodemann and Stohl, 2009; Scarchilli et al., 2010; Werner et al., 2001). TD shows a completely different pattern, with moisture sources shifted towards the Pacific sector of the Southern Ocean compared to Vostok and EDC (Fig. 4 and Appendix B). Moreover, especially for Vostok and much less for EDC, the back trajectory model diagnosed apparent moisture sources over the interior of Antarctica. These continental moisture sources are probably due to the passage of air masses over the Antarctic interior where they potentially gain moisture from sublimating surface snow and may increase  $^{17}\text{O}$ -excess at Vostok compared to EDC and TD.

- Different seasonality of precipitation at Vostok and EDC may change mean level and evolution of  $^{17}\text{O}$ -excess during the deglaciation. Indeed, Risi et al. (2010) showed that a change in the seasonality can have a significant influence on  $^{17}\text{O}$ -excess because of a mixing effect. Today, for both sites, the precipitation occurs all year round (Gallee and Gorodetskaya, 2010; Ekaykin et al., 2004) and the back trajectory analysis (Appendix B) revealed similar seasonalities for both sites. Another possibility, based on the MCIM, to explain the different  $^{17}\text{O}$ -excess levels is to invoke a strong change in the supersaturation dependency on temperature between Vostok and EDC. We have indeed mentioned in the last section that  $^{17}\text{O}$ -excess mean level and the dependency on local temperature are very sensitive to the tuning of the supersaturation through kinetic fractionation. To explain a difference of 17 ppm

between  $^{17}\text{O}$ -excess at Vostok and EDC, the supersaturation dependency on temperature should be smaller than the one used in Eq. (8):  $S = 1 - 0.001 T_c$  instead of  $1 - 0.0033 T_c$ . This explanation of site-specific  $S$  over the Antarctic plateau is rather tempting, since it also better explains, regarding the given tuning of the MCIM, the difference in  $d$ -excess observed between Vostok and EDC: it predicts a change of  $d$ -excess by 3.3 ‰ (instead of 2 ‰ which are given in Table 1) and is therefore in better agreement with the measured difference of 5.7 ‰.

- Furthermore, Vostok may be affected by local  $^{17}\text{O}$ -excess inputs such as clear sky precipitation (diamond dust) or stratospheric water vapour inputs (Stohl and Sodemann, 2009; Miller, 2008; Zahn et al., 1998). From the available results of Franz and Röckmann (2005) reporting a  $^{17}\text{O}$ -anomaly of  $0 \pm 1800$  ppm in lowermost stratospheric water vapour over Antarctica, stratospheric influence on tropospheric precipitation has been considered negligible (Landais et al., 2008b). Still, due to the large uncertainty of this result, the  $^{17}\text{O}$ -anomaly of water vapour from the stratosphere may be greater than zero and therefore may influence  $^{17}\text{O}$ -excess of precipitation at Vostok significantly. More studies should be performed to test the strength of stratospheric influence in Antarctica.
- The stability of  $^{17}\text{O}$ -excess observed at TD over the deglaciation is in agreement with the interpretation given by the MCIM. Over the deglaciation,  $\delta^{18}\text{O}$  increases from  $-40.5$  to  $-36.5$  ‰ and within this range  $^{17}\text{O}$ -excess does not depend on the choice of the supersaturation function (Fig. 3a). Following the interpretation of the MCIM, decreasing  $^{17}\text{O}$ -excess at TD would be attributed to an increase in  $\text{RH}_n$  at the OSR. The low  $^{17}\text{O}$ -excess at TD thus reflects high latitude OSR in the Austral Ocean, a finding which is supported by the back trajectory model (Appendix B). High latitude OSR, near the Antarctic coast, are marked by high  $\text{RH}_n$  ( $\approx 90$  % for present-day, source: NCEP <http://www.esrl.noaa.gov/>), and therefore we do not expect decreasing  $\text{RH}_n$  at the OSR of TD during the deglaciation. Furthermore, Risi et al. (2010) found, based on model outputs from PMIP2 (<http://pmip2.lsce.ipsl.fr/>), nearly unchanged distribution of  $\text{RH}_n$  in the Austral ocean between LGM and EH. Still, we did not explore the possible influence on  $\text{RH}_n$  due to a shift of the sea ice margins.

For the  $^{17}\text{O}$ -excess increase over the deglaciation at EDC, the MCIM would suggest a decrease of the source  $\text{RH}_n$  by 10 %, with  $S = 1 - 0.0033 T_c$  ( $S = 1 - 0.001 T_c$  would require a 20 % decrease of  $\text{RH}_n$ , which is far too important). The OSR for EDC is situated at lower latitudes than the OSR for TD, so an unequal variation of  $\text{RH}_n$  for two different OSRs in the Austral ocean during the deglaciation can not be excluded. A shift in  $\text{RH}_n$  of

10 % does not necessarily mean that the same OSR underwent such a change, since moisture origin of one site may be geographically different for EH and LGM. An increasing number of studies (Mc Glone et al., 2010; Lamy et al., 2010; Putnam et al., 2010) suggest major shifts in intensity and location of the southern westerlies during the last deglaciation. These changes may have modified the climatic conditions at the ocean surface as well as the location of the more important evaporation zones. Such effect could also explain the rapid  $d$ -excess shift, observed at EDC, at the end of Termination 2 (Masson-Delmotte et al., 2010) and has probably also an influence on  $^{17}\text{O}$ -excess. The lack of present-day equivalent for LGM conditions at Vostok, EDC and TD remains a limitation for solid interpretation of isotopic signals in these regions.

## 6 Summary and conclusion

We obtained  $^{17}\text{O}$ -excess records spanning the last deglaciation for the sites of Dome C (EDC) and of Talos Dome (TD) (East Antarctica) and compared these results with the first profile previously obtained from the Vostok ice core (Landais et al., 2008a). The data depict two important results:

- EH mean levels of  $^{17}\text{O}$ -excess are different for all three Antarctic ice core sites.
- The three sites are marked by different evolution of  $^{17}\text{O}$ -excess during the last deglaciation.

At EDC, which is marked by continental climatic conditions, we observed an increasing trend in  $^{17}\text{O}$ -excess, from 11 (LGM) to 23 (EH) ppm, hence smaller than the 20 ppm (LGM = 20 ppm, EH = 40 ppm) rise at Vostok. At TD, which is a more coastal site, a stable  $^{17}\text{O}$ -excess of 5 ppm was measured throughout the last deglaciation.

The different levels of  $^{17}\text{O}$ -excess between Vostok, EDC and TD at EH are consistent with unequal modern  $\text{RH}_n$  of the OSR, as expected from our current understanding of  $^{17}\text{O}$ -excess in polar regions. The lower  $^{17}\text{O}$ -excess for TD, compared to the one at EDC, reflects the influence of OSR from higher latitudes and therefore higher  $\text{RH}_n$  (Appendix B; Sodemann and Stohl, 2009; Scarchilli et al., 2010).

We explain the unequal evolution of  $^{17}\text{O}$ -excess for Vostok, EDC and TD respectively, with a different glacial/interglacial change in  $\text{RH}_n$  at their respective OSRs. Following this interpretation,  $\text{RH}_n$  of the OSR for TD remained almost constant, whereas for EDC it decreased by 10 %. A change in humidity conditions of the OSR for EDC may be linked to the modifications of strength and location of the westerlies (Mc Glone et al., 2010; Lamy et al., 2010).

From the MCIM (tuned for the transect study from Terra-Nova Bay to EDC) results, we conclude that  $^{17}\text{O}$ -excess can serve as marker of  $\text{RH}_n$  of the OSR in the coastal region of

Antarctica. For the remote continental sites of East Antarctica, we found that the dependence of  $^{17}\text{O}$ -excess on local temperature is highly sensitive to the choice of the supersaturation function  $S$ . Such effect is also true for  $d$ -excess. It follows that local effects may significantly contribute to the  $^{17}\text{O}$ -excess and  $d$ -excess signals at Vostok and to a lesser degree at EDC.

Finally, our work has two important consequences. First, it demonstrates that the previous  $^{17}\text{O}$ -excess profile measured at Vostok (during the last deglaciation) is a regional signal and should therefore not be interpreted as a decrease in  $\text{RH}_n$  of the Southern Ocean, as it has been suggested in Landais et al. (2008a); local effects such as changes in supersaturation or stratospheric inputs may be at play. Therefore, reconstructing past  $\text{RH}_n$  of the OSR is more reliable from coastal ice cores. Second, the particular sensitivity of  $^{17}\text{O}$ -excess to supersaturation should not be seen as a disadvantage for paleo climatic reconstruction:  $^{17}\text{O}$ -excess spatial distributions for different periods could help to constrain the supersaturation dependency on temperature and thus help to interpret climatic signals of  $\delta^{18}\text{O}$  and  $d$ -excess.

## 7 Outlook

$^{17}\text{O}$ -excess measurements on other sites, such as EPICA Dronning Maud Land, Law Dome and Berkner, will expand the spatial distribution of  $^{17}\text{O}$ -excess records in Antarctica and therefore could give constraints on the accurate tuning of the supersaturation function in the MCIM. The analysis of surface snow and of snowpits from Vostok will let us depict seasonal and inter annual variations of  $^{17}\text{O}$ -excess. The comparison of  $^{17}\text{O}$ -excess data, stemming from the Vostok site, with ice core proxies for stratospheric inputs (tritium,  $^{10}\text{Be}$ ), can help to quantify the influence of non-mass-dependent fractionation effects on  $^{17}\text{O}$ -excess. Isotopic analysis of surface snow and at the same time of the water vapour of the lowest atmosphere layer in polar regions should allow us to get information about post-deposit isotopic fractionation processes, such as local recycling due to evaporation/sublimation.

## Appendix A

### Statistics

#### A1 Two sample confidence bounds

In order to compare the two mean levels  $\mu_E$  and  $\mu_L$  of  $^{17}\text{O}$ -excess for EH and LGM, respectively, we computed a two sample confidence interval for their difference  $\mu_E - \mu_L$ , for the data of EDC and TD separately. For both ice core sites, we took samples of data points corresponding to the same period: The epoch of EH spans the period from 9 to 12 ka with data points  $E_1, E_2, \dots, E_n$ ; the epoch of LGM contains

the period from 20 to 25 ka with data points  $L_1, L_2, \dots, L_m$ . We estimated the unknown mean values  $\mu_E$  and  $\mu_L$  by the sample means  $\bar{E} = n^{-1} \sum_{i=1}^n E_i$  and  $\bar{L} = m^{-1} \sum_{i=1}^m L_i$ , respectively. With  $S_E$  and  $S_L$  denoting the corresponding sample standard deviations, one can compute the following two-sample confidence bounds for  $\mu_E - \mu_L$ :

$$\bar{E} - \bar{L} \pm \sqrt{\frac{n+m}{nm}} S t_{n+m-2;0.975} \quad (\text{A1})$$

$$S = \sqrt{\frac{(n-1)S_E^2 + (m-1)S_L^2}{n+m-2}} \quad (\text{A2})$$

where  $S$  corresponds to the estimated standard deviation of a single measurement, and  $t_{n+m-2;0.975}$  denotes the 97.5%-quantile of student's  $t$ -distribution, e.g. Papula (2001), with  $m+n-2$  degrees of freedom. With 95% confidence we may conclude that the unknown difference  $\mu_E - \mu_L$  is between these two confidence bounds. Using Eq. (A1), we end up with the confidence bounds 7.01 and 15.13 for EDC, so there is evidence that  $\mu_E - \mu_L$  is strictly greater than zero. For TD, the confidence bounds are  $-10.04$  and  $5.19$ , so there is no evidence for  $\mu_E - \mu_L$  being different from zero. In other words, the computation of the two-sample confidence bounds evidenced a significant increase in  $^{17}\text{O}$ -excess at EDC during the last deglaciation. For TD, the observed difference  $\bar{E} - \bar{L}$  was not significantly different from zero. Table A1 summarizes these results for EDC and TD.

#### A2 Regression analysis

To obtain a statistical tool to depict a possible trend in  $^{17}\text{O}$ -excess at EDC (as well at TD), we performed a regression analysis using the open source software *R* (R Development Core Team, 2011).

Generally we assume that the  $i$ -th measurement equals  $Y_i = f(X_i) + \epsilon_i$  for an unknown regression function  $f$  and measurement errors  $\epsilon_i$ , where  $X_i$  corresponds to the age in ka while  $i$  runs from 1 to 58 for EDC and from 1 to 44 for TD. Assuming a certain type of  $f$ , we estimated it via least squares as  $\hat{f}$ , and this fitted function yielded the residuals  $\hat{\epsilon}_i = Y_i - \hat{f}(X_i)$ . Scatter plots of the pairs  $(\hat{\epsilon}_i, \hat{\epsilon}_{i+1})$  showed no correlation, so we assumed the uncertainties  $\epsilon_i$  to be independent. Moreover, a normal QQ-plot of the residuals supported the assumption of the uncertainties being Gaussian, so we applied standard methodology for regression models.

First, we assumed a linear trend in  $^{17}\text{O}$ -excess for the considered period of the last deglaciation. That means we considered the family of all linear functions,  $f_{\text{lin}}(x) = a + bx$ , to explain our data of  $^{17}\text{O}$ -excess, where  $a$  is the ordinate intercept ( $=$   $^{17}\text{O}$ -excess at present),  $b$  the gradient of  $^{17}\text{O}$ -excess during the period from LGM to EH and  $x$  is the age in ka. In order to check if nonlinear functions with more degrees of freedom would fit our data more accurately, we performed F-tests of a linear trend versus the alternative hypothesis of a (i) quadratic function  $f$ , (ii) a cubic function  $f$

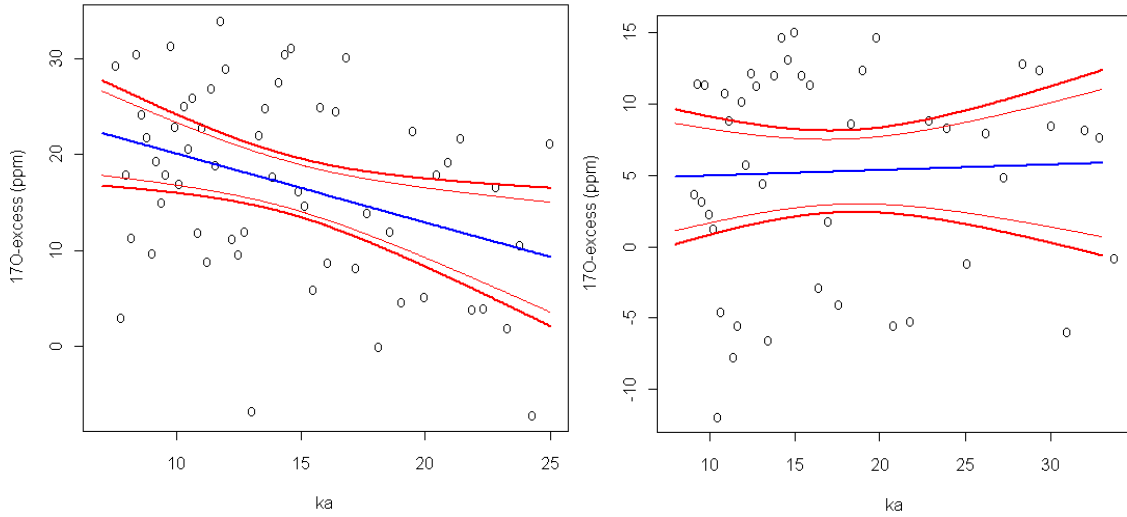


**Fig. A1.** (a) (left for EDC) and (b) (right for TD) show the results of linear regression analysis of the LGM-EH  $^{17}\text{O}$ -excess data (blue lines). The red lines are the point-wise and simultaneous 95 % confidence bounds.

**Table A1.** Result of the performed two-sample confidence bounds:  $\bar{E}$  and  $\bar{L}$  are the estimated sample means of the data corresponding to EH and LGM, respectively.  $S_E$  and  $S_L$  denote the corresponding sample standard deviations and  $S$  corresponds to the estimated (common) standard deviation of the single measurements.  $n$  and  $m$  are the number of samples taken into account for the periods of EH and LGM, respectively. The last column corresponds to the upper and lower confidence bounds, respectively: with 95 % confidence,  $\mu_E - \mu_L$  lies between the lower and upper value.

	Two-sample confidence bounds						$\mu_E - \mu_L$
	$\bar{E}$	$\bar{L}$	$S_E$	$S_L$	$n$	$m$	
Dome C (EDC)	23	11.9	3.65	5.98	13	12	$7.01 \leq \dots \leq 15.13$
Talos Dome (TD)	2.6	4.7	6.7	8.3	13	6	$-10.04 \leq \dots \leq 5.19$

and (iii) a cubic spline  $f$  with four knots. The high p-values of these F-tests ( $p(\text{i}) = 0.35$ ,  $p(\text{ii}) = 0.51$  and  $p(\text{iii}) = 0.84$ ) indicate that there is no evidence for a nonlinear trend of  $^{17}\text{O}$ -excess at EDC. The same conclusion is true for the regression analysis of  $^{17}\text{O}$ -excess at TD, where we obtained the following p-values of the F-tests:  $p(\text{i}) = 0.61$ ,  $p(\text{ii}) = 0.72$  and  $p(\text{iii}) = 0.44$ .

Table A2 displays the result of the linear regression analysis. There, the p-value is for the null hypotheses of no trend at all, i.e. a constant level of  $^{17}\text{O}$ -excess and  $b = 0$ . The very low p-value at EDC indicates that there is a significant linear increase of 12 ppm ( $\hat{f}_{\text{lin}}(\text{EH}) - \hat{f}_{\text{lin}}(\text{LGM}) = 0.72(-9 + 25) = 11.52$ ) during the last deglaciation. For TD, the regression analysis yields no significant temporal gradient during the period from 25 to 9 ka.

## Appendix B

### Results of the Lagrangian source diagnostics

Figure 4 shows the seasonal mean moisture sources as contribution to precipitation in the target area in units of  $\text{mm yr}^{-1}$  identified from the Lagrangian moisture source diagnostic of Sodemann et al. (2008) for the ice core drilling sites Vostok (a, b), EDC (c, d), and TD (e, f) for January-February-March (JFM, left column) and August-September-October (ASO, right column). Seasonal variation of the moisture origins is most pronounced between the time of minimum (JFM) and maximum (ASO) sea ice cover (Masson-Delmotte et al., 2011); hence, composites for these seasons are reported here as well. A  $3 \times 3$  degree smoothing has been applied to more clearly show the main characteristics of the moisture source pattern.

During SH summer, Vostok has most moisture sources in the Indian Ocean and the corresponding sector of the Southern Ocean (Fig. 4a and b). However, the moisture sources

**Table A2.** Result of the most robust regression function. The temporal gradient of  $^{17}\text{O}$ -excess is reproduced by the linear functions with the ordinate intercept  $a$  and the gradient  $b$ . Explanation of significance level: very high (p-value < 0.001), high (p-value < 0.01), significant (p-value < 0.05), perhaps (p-value < 0.1), not significant (p-value > 0.1).

	Linear regression functions			
	$a$	$b$	p-value	significance level
Dome C (EDC)	$27.3 \pm 3.76$	$0.72 \pm 0.24$	0.005	high
Talos Dome (TD)	$3.8 \pm 1.4$	$-0.14 \pm 0.07$	0.797	not significant

span a wide longitudinal range, and include significant contributions from the Southern Atlantic Ocean and the Pacific Ocean, and the corresponding sectors of the Southern Ocean. For EDC (Fig. 4c and d), the diagnosed moisture sources are qualitatively similar, but with markedly lower contributions from the Pacific and Atlantic sectors. At both sites, during SH winter the overall amount of advected moisture is higher, and moisture sources are more confined to local longitudes (Fig. 4 right panels). Being a lower-altitude site near the coast, TD has a different diagnosed pattern of moisture sources (Fig. 4e and f). Moisture sources are shifted towards the Pacific sector of the Southern Ocean compared to Vostok and EDC. The overall magnitude of diagnosed evaporation contribution is higher due to the lower elevation of the site.

There are notable apparent moisture sources for Vostok over the Antarctic continent and at coastal locations in East Antarctica (Fig. 4a). The moistening of air masses identified over the interior of Antarctica can be explained by the advection of moist air masses across West Antarctica to the Vostok site. Inspection of individual trajectories reveals that, in particular, moisture from the Atlantic and Pacific sectors is advected over the continental areas and experiences some moistening of the relatively dry air. It is not possible to decide whether the diagnosed moistening is a model artifact or whether it represents moisture fluxes from sublimating snow. However, the transport path associated with these air masses allows for more mixing of the advected air either with air masses near the surface or descending stratospheric air. This transport pathway seems to be a specific feature of the Vostok site, which is much less pronounced for the site EDC (Fig. 4b). For TD, no sources from the interior of the Antarctic continent are diagnosed (Fig. 4c), indicating that moist air masses are advected to the drilling site directly from the ocean. The diagnosed coastal moisture sources at all three sites possibly indicate moistening of the free troposphere due to boundary-layer venting as air masses encounter the steep orography of East Antarctica.

*Acknowledgements.* This work is a contribution to the European Project for Ice Coring in Antarctica (EPICA), a joint European Science Foundation/European Commission scientific programme, funded by the EU (EPICA-MIS) and by national contributions from Belgium, Denmark, France, Germany, Italy, the Netherlands,

Norway, Sweden, Switzerland and the United Kingdom. The Talos Dome Ice core Project (TALDICE), a joint European programme, is funded by national contributions from Italy, France, Germany, Switzerland and the United Kingdom. The work (fluorination, IRMS) done at LSCE is funded by the ANR CITRONNIER. We thank Françoise Vimeux for providing samples from the Vostok ice core, Eugeni Barkan for helping with the inter calibration between the IES and the LSCE, Ryu Uemura for the fruitful discussions and Martin Miller for the cross-read of the manuscript. Thanks also go to the Marie Curie Initial Training Network INTRAMIF (FP7), which has funded R. Winkler's PhD at LSCE-IPSL-CEA. This is LSCE-publication No. 4706 and TALDICE publication No. 15.

Edited by: V. Rath



The publication of this article is financed by CNRS-INSU.

## References

- Angert, A., Cappa, C. D., and Paolo, D. D.: Kinetic  $\delta^{17}\text{O}$  effects in the hydrological cycle: Indirect evidence and implications, *Geochim. Cosmochim. Acta*, 68, 3487–3495, 2004.
- Barkan, E. and Luz, B.: High precision measurements of  $^{17}\text{O}/^{16}\text{O}$  and  $^{18}\text{O}/^{16}\text{O}$  ratios in  $\text{H}_2\text{O}$ , *Rapid Comm. Mass Spect.*, 19, 3737–3742, 2005.
- Barkan, E. and Luz, B.: Diffusivity fractionations of  $\text{H}_2^{16}\text{O}/\text{H}_2^{17}\text{O}$  and  $\text{H}_2^{16}\text{O}/\text{H}_2^{18}\text{O}$  in air and their implications for isotope hydrology, *Rapid Comm. Mass Spect.*, 21, 2999–3005, 2007.
- Cappa, C., Hendricks, M. B., De Paolo, D. J., and Cohen, R.: Isotopic fractionation of water during evaporation, *J. Geophys. Res.*, 108, 4525–4535, 2003.
- Ciais, P. and Jouzel, J.: Deuterium and oxygen 18 in precipitation: Isotopic model, including mixed cloud processes, *J. Geophys. Res.*, 99, 16793–16803, 1994.
- Coplen, T. B.: Guidelines and recommended terms for expression of stable-isotope-ratio and gas-ratio measurement results, *Rapid Comm. Mass Spect.*, 25, 2538–2560, 2011.

- Craig, H.: Isotopic standards for carbon and oxygen and correction factors for mass spectrometric analysis of carbon dioxide, *Geochim. Cosmochim. Acta*, 12, 133–149, 1957.
- Craig, H.: Isotopic Variations in Meteoric Waters, *Science*, 133, 1702–1703, 1961.
- Craig, H. and Gordon, L.: Deuterium and oxygen 18 variations in the ocean and the marine atmosphere., Symposium on Marine Geochemistry, Narragansett Marine Laboratory, University of Rhode Island Publication, 3, 277–374, 1965.
- Dansgaard, W.: Stable isotopes in precipitation, *Tellus*, 169, 436–468, 1964.
- Delmotte, M., Masson, V., Jouzel, J., and Magon, V.: A seasonal deuterium excess signal at Law Dome, coastal Eastern Antarctica: A Southern ocean signature, *J. Geophys. Res.*, 105, 7187–7197, 2000.
- Ekaykin, A. and Lipenkov, V. Y.: Formation of the Ice Core Isotopic Composition, in: PICR II “Physics of Ice-Core Records”, edited by: Hondoh, T., Institute of Low Temperature Science, Hokkaido University Press, Sapporo, 299–314, 2009.
- Ekaykin, A. A., Lipenkov, V. Y., Kuzmina, I., Petit, J.-R., Masson-Delmotte, V., and Johnsen, S. J.: The changes in isotope composition and accumulation of snow at Vostok station, East Antarctica, over the past 200 years, *Ann. Glaciol.*, 39, 569–575, 2004.
- EPICA-Members: Eight glacial cycles from Antarctic ice core, *Nature*, 429, 623–628, 2004.
- Franz, P. and Röckmann, T.: High-precision isotope measurements of  $\text{H}_2^{16}\text{O}$ ,  $\text{H}_2^{17}\text{O}$  and  $\text{H}_2^{18}\text{O}$  and the  $\Delta^{17}\text{O}$ -anomaly of water vapour in the Southern lowermost stratosphere, 2005.
- Gallee, H. and Gorodetskaya, I.: Validation of a limited area model over Dome C, Antarctic Plateau, during winter, *Clim. Dynam.*, 34, 61–72, 2010.
- Gat, J. R. and Mook, W. G.: Stable Isotope processes in the water cycle, *Environmental Isotopes in the Hydrological cycle*, edited by: Mook, W. G., Chap. 3, U. N. Educ. Sci. and Cult. Org. IAEA, Paris, 2, 17–42, 1994.
- Johnsen, S., Dansgaard, W., and White, J.: The origin of Arctic precipitation under present and glacial conditions, *Tellus*, 41, 452–468, 1989.
- Jouzel, J. and Koster, R. D.: A reconsideration of the initial conditions used for stable water isotope models, *J. Geophys. Res.*, 101, 22933–22938, 1996.
- Jouzel, J. and Merlivat, L.: Deuterium and Oxygen 18 in precipitation: Modelling of the isotopic effects during snow formation, *J. Geophys. Res.*, 89, 11749–11757, 1984.
- Jouzel, J., Merlivat, L., and Lorius, C.: Deuterium excess in an East Antarctic ice core suggests higher normalized relative humidity at the oceanic surface during the last glacial maximum, *Nature*, 299, 688–691, 1982.
- Jouzel, J., Vimeux, F., Caillon, N., Delaygue, G., Hoffmann, G., Masson-Delmotte, V., and Parrenin, F.: Magnitude of isotope/temperature scaling for interpretation of Central Antarctic ice cores, *J. Geophys. Res.*, 108, 4361–4372, 2003.
- Jouzel, J., Masson-Delmotte, V., Cattani, O., Dreyfus, G., Falourd, S., Hoffmann, G., Minster, B., Nouet, J., Barnola, J., Chapellaz, J., Fischer, H., Gallet, J., Johnsen, S., Leuenberger, M., Loulergue, L., Luthi, D., Oerter, H., Parrenin, F., Raisbeck, G., Raynaud, D., Schilt, A., Schwander, J., Selmo, E., Souchez, R., Spahni, R., Stauffer, B., Steffensen, J., Stenni, B., Stocker, T., Tison, J., Werner, M., and Wolff, E.: Orbital and Millennial Antarctic Climate Variability over the Past 800 000 Years, *Science*, 317, 793(2007), doi:10.1126/science.1141038, 2007.
- Kaiser, J.: Technical note: Consistent calculation of aquatic gross production from oxygen triple isotope measurements, *Biogeochemistry*, 8, 1793–1811, doi:10.5194/bg-8-1793-2011, 2011.
- Kavanaugh, J. and Cuffey, K.: Space and time variation of  $\delta^{18}\text{O}$  and  $\text{dD}$  in Antarctic precipitation revisited, *Global Biogeochem. Cy.*, 17, 1017–1030, 2003.
- Laepple, T., Werner, M., and Lohmann, G.: Synchronicity of Antarctic temperatures and local solar insolation on orbital timescales, *Nature*, 471, 91–94, 2011.
- Lamy, F., Kilian, R., Arz, H. W., François, J.-P., Kaiser, J., Prange, M., and Steinke, T.: Holocene changes in the position and intensity of the Southern westerly wind belt, *Nat. Geosci.*, 3, 695–699, 2010.
- Landais, A., Barkan, E., and Luz, B.: Record of  $\delta^{18}\text{O}$  and  $^{17}\text{O}$ -excess in ice from Vostok Antarctica during the last 150 000 years, *Geophys. Res. Lett.*, 35, L02709–L02713, 2008a.
- Landais, A., Barkan, E., and Luz, B.: Reply to comment by Martin F. Miller on: Record of  $\delta^{18}\text{O}$  and  $^{17}\text{O}$ -excess in ice from Vostok Antarctica during the last 150 000 years, *Geophys. Res. Lett.*, 35, L23709, doi:10.1029/2008GL034694, 2008b.
- Landais, A., Steen-Larsen, H.-C., Guillevic, M., Masson-Delmotte, V., Vinther, B., and Winkler, R.: Isotopic composition of oxygen in surface snow and water vapour at NEEM, *Geochim. Cosmochim. Acta*, accepted, 2011.
- Landais, A., Barkan, E., Vimeux, F., Masson-Delmotte, V., and Luz, B.: Combined Analysis of Water Stable Isotope ( $\text{H}_2^{16}\text{O}$ ,  $\text{H}_2^{17}\text{O}$ ,  $\text{H}_2^{18}\text{O}$ ,  $\text{HD}^{16}\text{O}$ ), in: PICR II “Physics of Ice-Core Records”, edited by: Hondoh, T., Institute of Low Temperature Science, Hokkaido University Press, Sapporo, 315–327, 2009.
- Luz, B. and Barkan, E.: The isotopic ratios  $^{17}\text{O}/^{16}\text{O}$  and  $^{18}\text{O}/^{16}\text{O}$  in molecular oxygen and their significance in bio-geochemistry, *Geochim. Cosmochim. Acta.*, 69, 1099–1110, 2004.
- Luz, B. and Barkan, E.: Net and gross oxygen production from O-2/Ar, O-17/O-16 and O-18/O-16 ratios, *Aquat. Microb. Ecol.*, 56, 133–145, 2009.
- Luz, B., Barkan, E., Bender, M. L., Thiemens, M. H., and Boering, K. A.: Triple-isotope composition of atmospheric oxygen as a tracer of biosphere productivity, *Nature*, 400, 547–550, 1999.
- Luz, B., Barkan, E., Yam, R., and Shemesh, A.: Fractionation of oxygen and hydrogen isotopes in evaporating water, *Geochim. Cosmochim. Acta.*, 73, 6697–6703, 2009.
- Majoube, M.: Fractionnement en  $^{18}\text{O}$  entre l’eau et sa vapeur d’eau, *Journal Chem. Phys.*, 10, 1473, 1971a.
- Majoube, M.: Fractionnement en  $^{18}\text{O}$  entre la glace et la vapeur d’eau, *J. Climate Phys.*, 68, 625–636, 1971b.
- Masson-Delmotte, V., Stenni, B., and Jouzel, J.: Common millennial-scale variability of Antarctic and Southern Ocean temperatures during the past 5000 years reconstructed from the EPICA Dome C ice core, *Holocene*, 14, 145–151, 2004.
- Masson-Delmotte, V., Landais, A., Stievenard, M., Cattani, O., Falourd, S., Jouzel, J., Johnsen, S., Dahl-Jensen, D., Sveinbjornsdottir, A., White, J., and Popp, T.: Holocene climatic changes in Greenland: Different deuterium-excess signals at Greenland ice core project (GRIP) and NorthGRIP, *J. Geophys. Res.*, 110, D14102–D14116, 2005.
- Masson-Delmotte, V., Hou, S., Ekaykin, A., Jouzel, J., Aristarain, A., Bernardo, R., Bromwich, D., Cattani, O., Delmotte, M.,

- Falourd, S., Frezzotti, M., Gallée, H., Genoni, L., Isaksson, E., Landais, A., Helsen, M., Hoffmann, G., Lopez, J., Morgan, V., Motoyama, H., Noone, D., Oerter, H., Petit, J., Royer, A., Uemura, R., Schmidt, G., Schlosser, E., Simoes, J., Steig, E., Stenni, B., Stievenard, M., Van Den Broeke, M., Van de Waal, R., Van de Berg, W., Vimeux, F., and White, J.: A review of Antarctic surface snow isotopic composition: Observations, atmospheric circulation, and isotopic modeling, *J. Climate*, 21, 3359–3387, 2008.
- Masson-Delmotte, V., Stenni, B., Blunier, T., Cattani, O., Chapellaz, J., Cheng, H., Dreyfus, G., Edwards, R. L., Falourd, S., Govin, A., Kawamura, K., Johnsen, S., Jouzel, J., Landais, A., Lemieux-Dudon, B., Lourantou, A., Marshall, G., Minster, B., Mudelsee, M., Pol, K., Röthlisberger, R., Selmo, E., and Waelbroeck, C.: Abrupt change of Antarctic moisture origin at the end of Termination II, *PNAS*, 2010.
- Masson-Delmotte, V., Buiron, D., Ekaykin, A., Frezzotti, M., Gallée, H., Jouzel, J., Krinner, G., Landais, A., Motoyama, H., Oerter, H., Pol, K., Pollard, D., Ritz, C., Schlosser, E., Sime, L. C., Sodemann, H., Stenni, B., Uemura, R., and Vimeux, F.: A comparison of the present and last interglacial periods in six Antarctic ice cores, *Clim. Past*, 7, 397–423, doi:10.5194/cp-7-397-2011, 2011.
- Mc Glone, M., Turney, C. S. M., Wilmshurst, J. M., Renwick, J., and Pahnke, K.: Divergent trends in land and ocean temperature in the Southern Ocean over the past 18'000 years, *Nat. Geosci.*, 3, 622–626, 2010.
- Meijer, H. A. J. and Li, W. J.: The use of electrolysis for accurate  $\delta^{18}\text{O}$  and  $\delta^{17}\text{O}$  isotope measurements in water, *Isotopes Environ. Health Stud.*, 34, 349–369, 1998.
- Merlivat, L.: The Dependence of Bulk Evaporation Coefficients on Air-Water Interfacial Conditions as Determined by the Isotopic Method, *J. Geophys. Res.*, 83, 2977–2980, 1978.
- Merlivat, L. and Jouzel, J.: Global climatic interpretation of the deuterium-oxygen 18 relationship for precipitation, *J. Geophys. Res.*, 84, 5029–5033, 1979.
- Merlivat, L. and Nief, G.: Fractionnement isotopique lors des changements d'Etat solid-vapeur et liquide-vapeur de l'eau des températures inférieures à 0 degrés C., *Tellus*, 1, 1967.
- Miller, M. F.: Isotopic fractionation and the quantification of  $^{17}\text{O}$  anomalies in the oxygen three-isotope system: an appraisal and geochemical significance, *Geochim. Cosmochim. Ac.*, 66, 1881–1889, 2002.
- Miller, M. F.: Comment on “Record of  $\delta^{18}\text{O}$  and  $^{17}\text{O}$ -excess in ice from Vostok Antarctica during the last 150'000 years” by Amaelle Landais et al., *Geophys. Res. Lett.*, 35, L23709, doi:10.1029/2008GL034505, 2008.
- Mook, W.: Environmental Isotopes in the Hydrological Cycle: Introduction, UNESCO IAEA, Paris, 1, 1994.
- Mook, W. G. and Grootes, P. M.: The measuring procedure and corrections for the high precision mass spectrometric analysis of isotopic abundance ratios, especially referring to carbon, oxygen and nitrogen, *Int. J. Mass Spectrom. Ion Phys.*, 12, 273–298, 1973.
- Noone, D.: The influence of midlatitude and tropical overturning circulation on the isotopic composition of atmospheric water vapor and Antarctic precipitation, *J. Geophys. Res.*, 113, D04102–D04114, 2008.
- Papula, L.: Mathematik für Ingenieure und Naturwissenschaftler Band 3, Viewegs Fachbücher der Technik, Braunschweig Wiesbaden, 740 pp., 2001.
- Petit, J. R., White, J. W. C., Young, N. W., Jouzel, J., and Korotkevich, Y. S.: Deuterium Excess in recent Antarctic Snow, *J. Geophys. Res.*, 96, 5113–5122, 1991.
- Putnam, A. E., Denton, G. H., Schaefer, J. M., Barrell, D. J. A., Andersen, B. G., Finkel, R. C., Schwartz, R., Doughty, A. M., Kaplan, M. R., and Schlüchter, C.: Glacier advance in Southern middle-latitudes during the Antarctic Cold Reversal, *Nat. Geosci.*, 3, 700–704, 2010.
- R Development Core Team: R: A Language and Environment for Statistical Computing, R Foundation for Statistical Computing, Vienna, Austria, <http://www.R-project.org>, ISBN 3-900051-07-0, 2011.
- Risi, C., Landais, A., Bony, S., Jouzel, J., Masson-Delmotte, V., and Vimeux, F.: Understanding the  $^{17}\text{O}$ -excess glacial-interglacial variations in Vostok precipitation, *J. Geophys. Res.*, 115, D10112–D10126, 2010.
- Scarchilli, C., Frezzotti, M., and Ruti, P.: Snow precipitation at four ice core sites in East Antarctica: provenance, seasonality and blocking factors, *Clim. Dynam.*, 4, 946–964, 2010.
- Sodemann, H. and Stohl, A.: Asymmetries in the moisture origin of Antarctic precipitation, *Geophys. Res. Lett.*, 36, L22803–L22807, 2009.
- Sodemann, H., Schwierz, C., and Wernli, H.: Interannual variability of Greenland winter precipitation sources: Lagrangian moisture diagnostic and North Atlantic Oscillation influence, *Geophys. Res. Lett.*, 113, D03107–D03123, 2008.
- Stenni, B., Masson-Delmotte, V., Johnsen, S., Jouzel, J., Longinelli, A., Monnin, E., Röthlisberger, R., and Selmo, E.: An Oceanic Cold Reversal during the last deglaciation, *Science*, 293, 2074–2077, 2001.
- Stenni, B., Jouzel, J., Masson-Delmotte, V., Röthlisberger, R., Castellano, E., Cattani, O., Falourd, S., Johnsen, S. J., Longinelli, A., Sachs, J. P., Selmo, E., Souchez, R., Steffensen, J. P., and Udisti, R.: A late-glacial high-resolution site and source temperature record derived from the EPICA Dome C isotope records (East Antarctica), *Earth Planet. Sci. Lett.*, 217, 183–195, 2003.
- Stenni, B., Masson-Delmotte, V., Selmo, E., Oerter, H., Meyer, H., Röthlisberger, R., Jouzel, J., Cattani, O., Falourd, S., Fischer, H., Hoffmann, G., Iacumin, P., Johnsen, S. J., Minster, B., and Udisti, R.: The deuterium excess records of EPICA Dome C and Dronning Maud Land ice cores (East Antarctica), *Quaternary Sci. Rev.*, 29, 146–159, 2010.
- Stenni, B., Buiron, D., Frezzotti, M., Albani, S., Barbante, C., Bard, E., Barnola, J., Baroni, M., Baumgartner, M., Bonazza, M., Capron, E., Castellano, E., Chapellaz, J., Delmonte, B., Falourd, S., Genoni, L., Iacumin, P., Jouzel, J., Kipfstuhl, S., Landais, A., Lemieux-Dudon, B., Maggi, V., Masson-Delmotte, V., Mazzola, C., Minster, B., Montagnat, M., Mulvaney, R., Narcisi, B., Oerter, H., Parrenin, F., Petit, J., Ritz, C., Scarchilli, C., Schilt, A., Schübbach, S., Schwander, J., Selmo, E., Stocker, T., and Udisti, R.: Expression of the bipolar sea-saw in Antarctic climate records during the last deglaciation, *Nat. Geosci.*, 4, 46–49, 2011.
- Stohl, A. and Sodemann, H.: Characteristics of the atmospheric transport into the Antarctic troposphere, *J. Geophys. Res.*, D02305–D02320, 2009.
- Stohl, A., Forster, C., Frank, A., Seibert, P., and Wotawa,

- G.: Technical note: The Lagrangian particle dispersion model FLEXPART version 6.2, *Atmos. Chem. Phys.*, 5, 2461–2474, doi:10.5194/acp-5-2461-2005, 2005.
- Uemura, R., Barkan, E., Abe, O., and Luz, B.: Triple isotopic composition of oxygen in atmospheric water vapor, *Geophys. Res. Lett.*, 37, L04402–L04405, 2010.
- Van Hook, W. A.: Vapour Pressures of Isotopic Waters and Ices, *J. Phys. Chem.-US*, 72, 1234–1244, 1968.
- Vimeux, F., Masson, V., Jouzel, J., Stievenard, M., and Petit, J. R.: Glacial-interglacial changes in the ocean surface conditions in the Southern Hemisphere, *Nature*, 398, 410–413, 1999.
- Vimeux, F., Masson, V., Delaygue, G., Jouzel, J., Petit, J. R., and Stievenard, M.: A 420,000 year deuterium excess record from East Antarctica: Information on past changes in the origin of precipitation at Vostok, *J. Geophys. Res.*, 106, 31863–31873, 2001.
- Vimeux, F., Cuffey, K. M., and Jouzel, J.: New insights into Southern Hemisphere temperature changes from Vostok ice cores using deuterium excess correction, *Earth Planet. Sci. Lett.*, 203, 829–843, 2002.
- Werner, M., Heimann, M., and Hoffmann, G.: Isotopic composition and origin of polar precipitation in present and glacial climate simulations, *Tellus*, 53, 53–71, 2001.
- Zahn, A., Barth, V., Pfeilsticker, K., and Platt, U.: Deuterium, Oxygen-18 and Tritium as tracers for water vapour transport in the lower stratosphere and tropopause region., *Journal Atmos. Chem.*, 30, 25–47, 1998.